

Chapter 10

Dynamic Analysis of the Vehicle-Track Coupling System with Finite Elements in a Moving Frame of Reference

With the rapid development of high-speed railways and passenger-dedicated lines, train speed is remarkably improved, and slab track has been the main form for high-speed railways. With giant economic benefit, large increase in railway running speed leads to the adding of wheel-rail interaction, and the vibration noise problem emerges. Slab track structure is a new type of track structure and is very different from the conventional ballast track.

The research of above problems needs the support of dynamics, and therefore it is of great importance to study the effective algorithm of the dynamics in vehicle-track coupling system. Scholars at home and abroad have done huge research in this field. Crassie et al. [1] in Cambridge University have studied the dynamic response of railway track to high frequency vertical excitation; Eisenmann [2] from Munich Engineering & Technology University proposes multi-level theory of ballastless track and applies it into the structure design and load measuring. Chinese Professor Zhai [3, 4] sets up a model of vehicle-track coupling dynamic system and puts it into the study of ballastless track dynamics. Xiang and Zeng [5, 6] propose the principle of “set in the right position” for establishing the dynamic equation of the vehicle-track coupling system and the corresponding matrix assembling method. Lei et al. [7, 8] develop a vibration analysis model and its cross iteration algorithm for the train-track-subgrade nonlinear coupling system with finite element. Xie [9] studies the dynamic response of Winkler beam under a moving load. Koh [10] from Singapore State University proposes moving element method and conducts dynamics analysis of a simplified rail model.

The above mentioned works treat rail beams as continuum and employ some analytical or numerical means to solve the governing differential equations. Furthermore, some boundary conditions have to be introduced artificially to truncate the infinitely long beam at both ends. The moving vehicle will soon come close to the artificial boundary end on the “downstream” side and may even go beyond the artificial boundary end. The numerical solution near the downstream boundary has to be ignored.

In this chapter, finite elements in a moving frame of reference will be used in the dynamic analysis of the train-slab track coupling system. By establishing the three-layer beam model of the slab track, the element mass, damping, and stiffness matrixes of the slab track in a moving frame of reference are deduced. The research in this chapter adopts the whole vehicle model in Chap. 9, and realizes coupling of the train and the track structure by equilibrium conditions of wheel-rail contact forces and geometrical compatibility conditions, which can effectively avoid the effect from the boundary on the calculated results, thus improving the computation efficiency.

10.1 Basic Assumptions

To establish the three-layer beam element model of CRTS II slab track, it is assumed:

- (1) Only vertical vibration effect of the vehicle-track coupling system is considered.
- (2) Linear elastic contact between the wheel and the rail is considered
- (3) Since the vehicle and the slab track are bilaterally symmetrical about the centerline of the track, only half of the coupling system is used for ease of calculation.
- (4) Rails are regarded as 2D beam element with continuous viscoelastic support. The stiffness coefficient and damping coefficient of the rail pads and fasteners are denoted as k_r and c_r , respectively.
- (5) Precast track slabs are discretized into 2D beam element with continuous viscoelastic support. The stiffness coefficient and damping coefficient of the cement asphalt mortar layer under the precast track slab are denoted as k_s and c_s , respectively.
- (6) The concrete support layer is discretized into 2D beam element with continuous viscoelastic support. The stiffness coefficient and damping coefficient of the subgrade under concrete supporting layer are denoted as k_h and c_h , respectively.
- (7) Only the middle part of the track slab is discussed; as for the two sides of the track slab, their related matrixes can be deduced with the same method.

10.2 Three-Layer Beam Element Model of the Slab Track in a Moving Frame of Reference

The geometry size of the slab track refers to Fig. 10.1. Figure 10.2 is the simplified three-layer continuous beam model of the slab track.

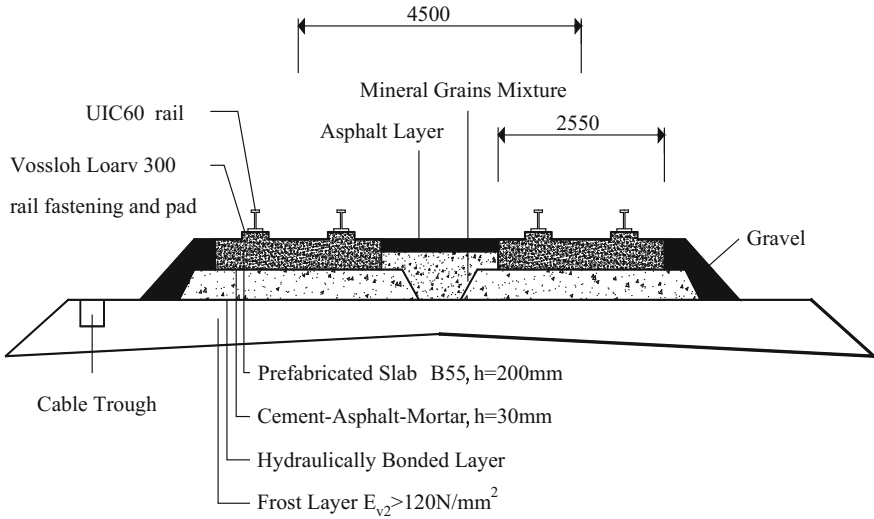


Fig. 10.1 CRTS II slab track

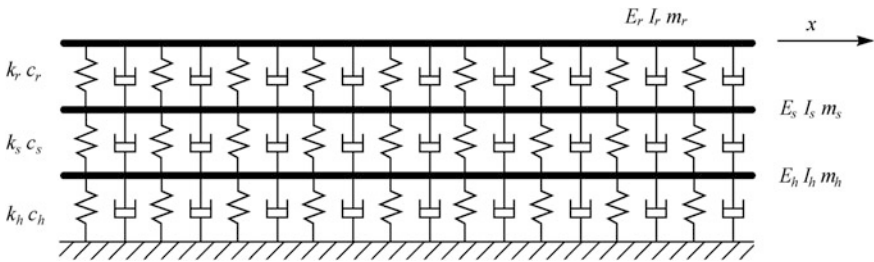


Fig. 10.2 Three-layer continuous beam model of the slab track

In Fig. 10.2, E_r , E_s , and E_h denote the elasticity modulus of the rail, the track slab, and the concrete support layer; I_r , I_s , and I_h denote the moment inertia of the rail, the track slab, and the concrete support layer; m_r , m_s , and m_h denote the mass of unit length of the rail, the track slab, and the concrete support layer.

10.2.1 Governing Equation of the Slab Track

As shown in Fig. 10.3, the dynamic analysis model of the vehicle-track coupling system is divided into upper vehicle subsystem and lower slab track subsystem. The vehicle moves along the track x direction at the speed of V .

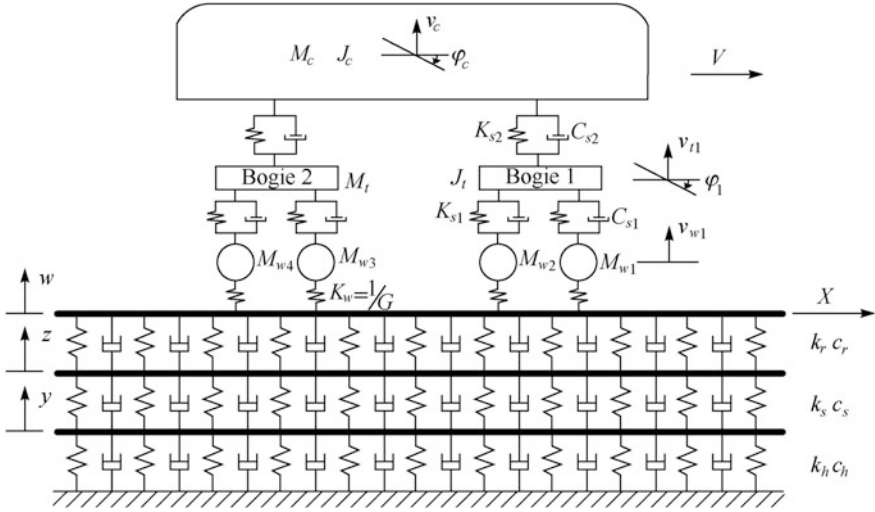


Fig. 10.3 Dynamic analysis model of the vehicle-track coupling system

The vertical vibration displacements of the rail, the precast track slab, and the concrete support layer are defined as w , z and y , and the governing equations of the slab track subsystems are as follows:

$$E_r I_r \frac{\partial^4 w}{\partial x^4} + m_r \frac{\partial^2 w}{\partial t^2} + c_r \left(\frac{\partial w}{\partial t} - \frac{\partial z}{\partial t} \right) + k_r (w - z) = F(t) \delta(x - Vt) \quad (10.1)$$

$$E_s I_s \frac{\partial^4 z}{\partial x^4} + m_s \frac{\partial^2 z}{\partial t^2} + c_s \left(\frac{\partial z}{\partial t} - \frac{\partial y}{\partial t} \right) - c_r \left(\frac{\partial w}{\partial t} - \frac{\partial z}{\partial t} \right) + k_s (z - y) - k_r (w - z) = 0 \quad (10.2)$$

$$E_h I_h \frac{\partial^4 y}{\partial x^4} + m_h \frac{\partial^2 y}{\partial t^2} + c_h \frac{\partial y}{\partial t} - c_s \left(\frac{\partial z}{\partial t} - \frac{\partial y}{\partial t} \right) + k_h y - k_s (z - y) = 0 \quad (10.3)$$

where $F(t)$ is the dynamic load at the wheel-rail contact point, δ is the Dirac delta function, x is the stationary coordinate in the longitudinal direction of the track, and its origin is arbitrary. For convenience, the origin is usually chosen at the endpoint of the left boundary.

Figure 10.4 shows the truncation of the slab track and the discretization into a finite number of moving elements (not necessarily of equal length) for the numerical modeling. Both the upstream and downstream ends of the truncated track are taken to be sufficiently far from the contact force such that their end forces and moments are zero.

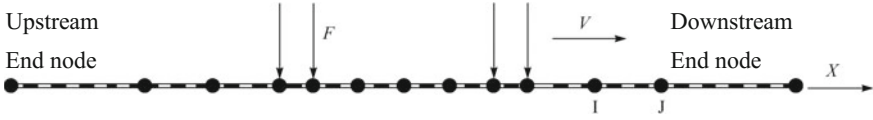


Fig. 10.4 Discretization of the slab track into moving elements

Consider a typical moving element of length l with node I and node J , a moving coordinate can be defined as follows:

$$r = x - x_I - Vt \quad (10.4)$$

where x_I is the stationary coordinate of node I . Accordingly, the origin of the r coordinate moves with the moving force/vehicle. Substituting this simple transformation into Eqs. (10.1)–(10.3), the governing equations for the three-layer beam model of the slab track subsystem in a moving frame of reference are

$$\begin{aligned} E_r I_r \frac{\partial^4 w}{\partial r^4} + m_r \left[V^2 \left(\frac{\partial^2 w}{\partial r^2} \right) - 2V \left(\frac{\partial^2 w}{\partial r \partial t} \right) + \left(\frac{\partial^2 w}{\partial t^2} \right) \right] + c_r \left[\left(\frac{\partial w}{\partial t} \right) - V \left(\frac{\partial w}{\partial r} \right) \right] \\ - c_r \left[\left(\frac{\partial z}{\partial t} \right) - V \left(\frac{\partial z}{\partial r} \right) \right] + k_r (w - z) = F(t) \delta(r + x_I) \end{aligned} \quad (10.5)$$

$$\begin{aligned} E_s I_s \frac{\partial^4 z}{\partial r^4} + m_s \left[V^2 \left(\frac{\partial^2 z}{\partial r^2} \right) - 2V \left(\frac{\partial^2 z}{\partial r \partial t} \right) + \left(\frac{\partial^2 z}{\partial t^2} \right) \right] + c_s \left[\left(\frac{\partial z}{\partial t} \right) - V \left(\frac{\partial z}{\partial r} \right) \right] \\ - c_s \left[\left(\frac{\partial y}{\partial t} \right) - V \left(\frac{\partial y}{\partial r} \right) \right] - c_r \left[\left(\frac{\partial w}{\partial t} \right) - V \left(\frac{\partial w}{\partial r} \right) \right] + c_r \left[\left(\frac{\partial z}{\partial t} \right) - V \left(\frac{\partial z}{\partial r} \right) \right] \\ + k_s (z - y) - k_r (w - z) = 0 \end{aligned} \quad (10.6)$$

$$\begin{aligned} E_h I_h \frac{\partial^4 y}{\partial r^4} + m_h \left[V^2 \left(\frac{\partial^2 y}{\partial r^2} \right) - 2V \left(\frac{\partial^2 y}{\partial r \partial t} \right) + \left(\frac{\partial^2 y}{\partial t^2} \right) \right] + c_h \left[\left(\frac{\partial y}{\partial t} \right) - V \left(\frac{\partial y}{\partial r} \right) \right] \\ - c_s \left[\left(\frac{\partial z}{\partial t} \right) - V \left(\frac{\partial z}{\partial r} \right) \right] + c_s \left[\left(\frac{\partial y}{\partial t} \right) - V \left(\frac{\partial y}{\partial r} \right) \right] + k_h y - k_s (z - y) = 0 \end{aligned} \quad (10.7)$$

Note that most of the elements do not have contact with the vehicle system. For such elements, the force term on the right-hand side of Eq. (10.5) is zero.

10.2.2 Element Mass, Damping, and Stiffness Matrixes of the Slab Track in a Moving Frame of Reference

As shown in Fig. 10.5 for a typical slab track element in a moving frame of reference, v_1, v_4 stand for vertical displacement of the rail, θ_1, θ_4 are the rotational angles of the rail; v_2, v_5 are the vertical displacements of the track slab, θ_2, θ_5 are the rotational angles of the track slab; v_3, v_6 are the vertical displacements of the concrete support layer; θ_3, θ_6 are the rotational angles of the concrete support layer.

Each slab track element in a moving frame of reference has 12 degrees of freedom. Defining the element node displacement vector as follows:

$$\mathbf{a}^e = \{v_1 \ \theta_1 \ v_2 \ \theta_2 \ v_3 \ \theta_3 \ v_4 \ \theta_4 \ v_5 \ \theta_5 \ v_6 \ \theta_6\}^T \quad (10.8)$$

The displacement at any point of the rail can be represented by interpolation function.

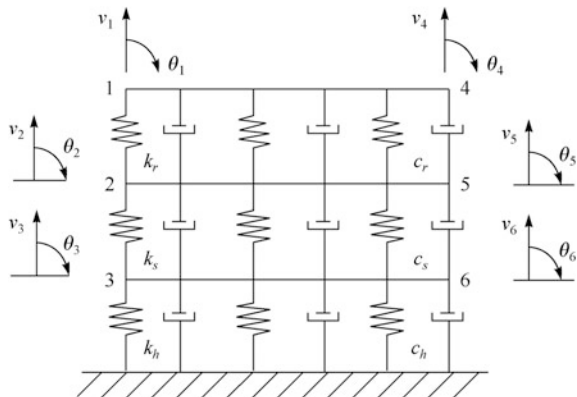
$$\begin{aligned} w &= N_1 v_1 + N_2 \theta_1 + N_3 v_4 + N_4 \theta_4 \\ &= [N_1 \ N_2 \ 0 \ 0 \ 0 \ 0 \ N_3 \ N_4 \ 0 \ 0 \ 0 \ 0] \mathbf{a}^e \\ &= \mathbf{N}_r \mathbf{a}^e \end{aligned} \quad (10.9)$$

where \mathbf{N}_r is the interpolation function matrix of the rail displacement, $N_1 - N_4$ are the displacement interpolation functions of the slab track element.

$$\begin{aligned} N_1 &= 1 - \frac{3}{l^2} r^2 + \frac{2}{l^3} r^3 & N_2 &= -r + \frac{2}{l} r^2 - \frac{1}{l^2} r^3 \\ N_3 &= \frac{3}{l^2} r^2 - \frac{2}{l^3} r^3 & N_4 &= \frac{1}{l} r^2 - \frac{1}{l^2} r^3 \end{aligned} \quad (10.10)$$

In the same way, the displacement at any point of the precast slab is as follows:

Fig. 10.5 CRTS II slab track element model



$$\begin{aligned}
z &= N_1 v_2 + N_2 \theta_2 + N_3 v_5 + N_4 \theta_5 \\
&= [0 \ 0 \ N_1 \ N_2 \ 0 \ 0 \ 0 \ 0 \ N_3 \ N_4 \ 0 \ 0] \mathbf{a}^e \quad (10.11) \\
&= \mathbf{N}_s \mathbf{a}^e
\end{aligned}$$

where, \mathbf{N}_s is the interpolation function matrix of the track slab displacement.

The displacement at any point of the concrete supporting layer is as follows:

$$\begin{aligned}
y &= N_1 v_3 + N_2 \theta_3 + N_3 v_6 + N_4 \theta_6 \\
&= [0 \ 0 \ 0 \ 0 \ N_1 \ N_2 \ 0 \ 0 \ 0 \ 0 \ N_3 \ N_4] \mathbf{a}^e \quad (10.12) \\
&= \mathbf{N}_h \mathbf{a}^e
\end{aligned}$$

where, \mathbf{N}_h is the interpolation function matrix of the concrete support layer displacement.

10.2.2.1 The First-Layer Beam's Matrix of the Slab Track Element in a Moving Frame of Reference

The governing equation (10.5) is multiplied by a weighting function (variation) w , and then integrated over the element length, leading to the variational (or weak) form as follows:

$$\begin{aligned}
&\int_0^l w(r) \left\{ E_r I_r \frac{\partial^4 w}{\partial r^4} + m_r \left[v^2 \left(\frac{\partial^2 w}{\partial r^2} \right) - 2V \left(\frac{\partial^2 w}{\partial r \partial t} \right) + \left(\frac{\partial^2 w}{\partial t^2} \right) \right] + c_r \left[\left(\frac{\partial w}{\partial t} \right) - V \left(\frac{\partial w}{\partial r} \right) \right] \right. \\
&\quad \left. - c_r \left[\left(\frac{\partial z}{\partial t} \right) - V \left(\frac{\partial z}{\partial r} \right) \right] + k_r (w - z) - F(t) \delta(r) \right\} dr = 0 \quad (10.13)
\end{aligned}$$

Take the integration to each term of above equation by parts over the element length l , namely:

$$\begin{aligned}
\int_0^l w(r) E_r I_r \frac{\partial^4 w}{\partial r^4} dr &= E_r I_r \int_0^l w(r) d \left(\frac{\partial^3 w}{\partial r^3} \right) = E_r I_r \left[\left(w(r) \cdot \frac{\partial^3 w}{\partial r^3} \right)_o^l - \int_0^l \frac{\partial^3 w}{\partial r^3} \cdot \frac{\partial w}{\partial r} dr \right] \\
&= -E_r I_r \int_0^l \frac{\partial w}{\partial r} d \left(\frac{\partial^2 w}{\partial r^2} \right) = -E_r I_r \left[\left(\frac{\partial w}{\partial r} \cdot \frac{\partial^2 w}{\partial r^2} \right)_o^l - \int_0^l \frac{\partial^2 w}{\partial r^2} \cdot \frac{\partial^2 w}{\partial r^2} dr \right] \\
&= E_r I_r \int_0^l (\mathbf{N}_{r,rr} \mathbf{a}^e)^T (\mathbf{N}_{r,rr} \mathbf{a}^e) dr = (\mathbf{a}^e)^T \cdot E_r I_r \int_0^l \mathbf{N}_{r,rr}^T \mathbf{N}_{r,rr} dr \cdot (\mathbf{a}^e) \quad (10.14)
\end{aligned}$$

$$\begin{aligned}
\int_0^l w(r) m_r V^2 \frac{\partial^2 w}{\partial r^2} dr &= m_r V^2 \int_0^l w(r) \frac{\partial^2 w}{\partial r^2} dr \\
&= m_r V^2 \int_0^l w(r) d\left(\frac{\partial w}{\partial r}\right) = m_r V^2 \left[\left(w(r) \cdot \frac{\partial w}{\partial r} \right)_o^l - \int_0^l \frac{\partial w}{\partial r} \cdot \frac{\partial w}{\partial r} dr \right] \\
&= -m_r V^2 \int_0^l (N_{r,r} \mathbf{a}^e)^T (N_{r,r} \mathbf{a}^e) dr = -(\mathbf{a}^e)^T \cdot m_r V^2 \int_0^l N_r^T N_r dr \cdot (\mathbf{a}^e)
\end{aligned} \tag{10.15}$$

$$\begin{aligned}
-2 \int_0^l w(r) m_r V \left(\frac{\partial^2 w}{\partial r \partial t} \right) dr &= -2 m_r V \int_0^l w(r) \left(\frac{\partial^2 w}{\partial r \partial t} \right) dr \\
&= -2 m_r V \int_0^l (N_r \mathbf{a}^e)^T (N_{r,r} \dot{\mathbf{a}}^e) dr \\
&= -(\mathbf{a}^e)^T \cdot 2 m_r V \int_0^l N_r^T N_r dr \cdot (\dot{\mathbf{a}}^e)
\end{aligned} \tag{10.16}$$

$$\begin{aligned}
\int_0^l w(r) m_r \left(\frac{\partial^2 w}{\partial t^2} \right) dr &= m_r \int_0^l w(r) \left(\frac{\partial^2 w}{\partial t^2} \right) dr \\
&= m_r \int_0^l w(r) \left(\frac{\partial^2 w}{\partial t^2} \right) dr = m_r \int_0^l (N_r \mathbf{a}^e)^T (N_r \ddot{\mathbf{a}}^e) dr \\
&= (\mathbf{a}^e)^T \cdot m_r \int_0^l N_r^T N_r dr \cdot (\ddot{\mathbf{a}}^e)
\end{aligned} \tag{10.17}$$

$$\begin{aligned}
\int_0^l w(r) c_r \left(\frac{\partial w}{\partial t} \right) dr &= c_r \int_0^l w(r) \left(\frac{\partial w}{\partial t} \right) dr = c_r \int_0^l (N_r \mathbf{a}^e)^T (N_r \dot{\mathbf{a}}^e) dr \\
&= (\mathbf{a}^e)^T \cdot c_r \int_0^l N_r^T N_r dr \cdot (\dot{\mathbf{a}}^e)
\end{aligned} \tag{10.18}$$

$$\begin{aligned}
& - \int_0^l w(r) c_r V \left(\frac{\partial w}{\partial r} \right) dr = -c_r V \int_0^l w(r) \left(\frac{\partial w}{\partial r} \right) dr \\
& = -c_r V \int_0^l (\mathbf{N}_r \mathbf{a}^e)^T (\mathbf{N}_{r,r} \mathbf{a}^e) dr \\
& = -(\mathbf{a}^e)^T \cdot c_r V \int_0^l \mathbf{N}_r^T \mathbf{N}_{r,r} dr \cdot (\mathbf{a}^e)
\end{aligned} \tag{10.19}$$

$$\begin{aligned}
& - \int_0^l w(r) c_r \left(\frac{\partial z}{\partial t} \right) dr = -c_r \int_0^l w(r) \left(\frac{\partial z}{\partial t} \right) dr \\
& = -c_r \int_0^l (\mathbf{N}_r \mathbf{a}^e)^T (\mathbf{N}_s \dot{\mathbf{a}}^e) dr = -(\mathbf{a}^e)^T \cdot c_r \int_0^l \mathbf{N}_r^T \mathbf{N}_s dr \cdot (\dot{\mathbf{a}}^e)
\end{aligned} \tag{10.20}$$

$$\begin{aligned}
& \int_0^l w(r) c_r V \left(\frac{\partial z}{\partial r} \right) dr = c_r V \int_0^l w(r) \left(\frac{\partial z}{\partial r} \right) dr \\
& = c_r V \int_0^l (\mathbf{N}_r \mathbf{a}^e)^T (\mathbf{N}_{s,r} \mathbf{a}^e) dr = (\mathbf{a}^e)^T \cdot c_r V \int_0^l \mathbf{N}_r^T \mathbf{N}_{s,r} dr \cdot (\mathbf{a}^e)
\end{aligned} \tag{10.21}$$

$$\begin{aligned}
& \int_0^l w(r) k_r w(r) dr = k_r \int_0^l w(r)^2 dr = k_r \int_0^l (\mathbf{N}_r \mathbf{a}^e)^T (\mathbf{N}_r \mathbf{a}^e) dr \\
& = (\mathbf{a}^e)^T \cdot k_r \int_0^l \mathbf{N}_r^T \mathbf{N}_r dr \cdot (\mathbf{a}^e)
\end{aligned} \tag{10.22}$$

$$\begin{aligned}
& - \int_0^l w(r) k_r z(r) dr = -k_r \int_0^l w(r) z(r) dr = -k_r \int_0^l (\mathbf{N}_r \mathbf{a}^e)^T (\mathbf{N}_s \mathbf{a}^e) dr \\
& = -(\mathbf{a}^e)^T \cdot k_r \int_0^l \mathbf{N}_r^T \mathbf{N}_s dr \cdot (\mathbf{a}^e)
\end{aligned} \tag{10.23}$$

By using the principle of the energy, the first-layer beam's mass, damping, and stiffness matrices of the slab track element in a moving frame of reference can be obtained as follows:

$$\mathbf{m}_r^e = m_r \int_0^l \mathbf{N}_r^T \mathbf{N}_r dr \quad (10.24)$$

$$\mathbf{c}_r^e = -2m_r V \int_0^l \mathbf{N}_r^T \mathbf{N}_{r,t} dr + c_r \int_0^l \mathbf{N}_r^T \mathbf{N}_r dr - c_r \int_0^l \mathbf{N}_r^T \mathbf{N}_s dr \quad (10.25)$$

$$\begin{aligned} \mathbf{k}_r^e = & E_r I_r \int_0^l \mathbf{N}_{r,rr}^T \mathbf{N}_{r,rr} dr - m_r V^2 \int_0^l \mathbf{N}_{r,rt}^T \mathbf{N}_{r,rt} dr - c_r V \int_0^l \mathbf{N}_r^T \mathbf{N}_{r,r} dr \\ & + c_r V \int_0^l \mathbf{N}_r^T \mathbf{N}_{s,r} dr + k_r \int_0^l \mathbf{N}_r^T \mathbf{N}_r dr - k_r \int_0^l \mathbf{N}_r^T \mathbf{N}_s dr \end{aligned} \quad (10.26)$$

10.2.2.2 The Second-Layer Beam's Matrix of the Slab Track Element in a Moving Frame of Reference

The governing equation (10.6) is multiplied by a weighting function (variation) z , and then integrated over the element length, leading to the variational (or weak) form as follows:

$$\begin{aligned} \int_0^l z(r) \left\{ E_s I_s \frac{\partial^4 z}{\partial r^4} + m_s \left[V^2 \left(\frac{\partial^2 z}{\partial r^2} \right) - 2V \left(\frac{\partial^2 z}{\partial r \partial t} \right) + \left(\frac{\partial^2 z}{\partial t^2} \right) \right] + c_s \left[\left(\frac{\partial z}{\partial t} \right) - V \left(\frac{\partial z}{\partial r} \right) \right] \right. \\ \left. - c_s \left[\left(\frac{\partial y}{\partial t} \right) - V \left(\frac{\partial y}{\partial r} \right) \right] - c_r \left[\left(\frac{\partial w}{\partial t} \right) - V \left(\frac{\partial w}{\partial r} \right) \right] + c_r \left[\left(\frac{\partial z}{\partial t} \right) - V \left(\frac{\partial z}{\partial r} \right) \right] + k_s (z - y) - k_r (w - z) \right\} dr = 0 \end{aligned} \quad (10.27)$$

Take the integration to each term of above equation by parts over the element length l , namely:

$$\begin{aligned}
& \int_0^l z(r) E_s I_s \frac{\partial^4 z}{\partial r^4} dr = E_s I_s \int_0^l z(r) d \left(\frac{\partial^3 z}{\partial r^3} \right) \\
& = E_s I_s \left[\left(z(r) \cdot \frac{\partial^3 z}{\partial r^3} \right)_o^l - \int_0^l \frac{\partial^3 z}{\partial r^3} \cdot \frac{\partial z}{\partial r} dr \right] = -E_s I_s \int_0^l \frac{\partial z}{\partial r} d \left(\frac{\partial^2 z}{\partial r^2} \right) \\
& = -E_s I_s \left[\left(\frac{\partial z}{\partial r} \cdot \frac{\partial^2 z}{\partial r^2} \right)_o^l - \int_0^l \frac{\partial^2 z}{\partial r^2} \cdot \frac{\partial^2 z}{\partial r^2} dr \right] \\
& = E_s I_s \int_0^l (\mathbf{N}_{s,r} \mathbf{a}^e)^T (\mathbf{N}_{s,r} \mathbf{a}^e) dr = (\mathbf{a}^e)^T \cdot E_s I_s \int_0^l \mathbf{N}_{s,r}^T \mathbf{N}_{s,r} dr \cdot (\mathbf{a}^e)
\end{aligned} \tag{10.28}$$

$$\begin{aligned}
& \int_0^l z(r) m_s V^2 \left(\frac{\partial^2 z}{\partial r^2} \right) dr = m_s V^2 \int_0^l z(r) \left(\frac{\partial^2 z}{\partial r^2} \right) dr \\
& = m_s V^2 \int_0^l z(r) d \left(\frac{\partial z}{\partial r} \right) = m_s V^2 \left[\left(z(r) \cdot \frac{\partial z}{\partial r} \right)_o^l - \int_0^l \frac{\partial z}{\partial r} \cdot \frac{\partial z}{\partial r} dr \right] \\
& = -m_s V^2 \int_0^l (\mathbf{N}_{s,r} \mathbf{a}^e)^T (\mathbf{N}_{s,r} \mathbf{a}^e) dr = -(\mathbf{a}^e)^T \cdot m_s V^2 \int_0^l \mathbf{N}_{s,r}^T \mathbf{N}_{s,r} dr \cdot (\mathbf{a}^e)
\end{aligned} \tag{10.29}$$

$$\begin{aligned}
& -2 \int_0^l m_s V z(r) \left(\frac{\partial^2 z}{\partial r \partial t} \right) dr = -2 m_s V \int_0^l z(r) \left(\frac{\partial^2 z}{\partial r \partial t} \right) dr \\
& = -2 m_s V \int_0^l (\mathbf{N}_s \mathbf{a}^e)^T (\mathbf{N}_{s,r} \dot{\mathbf{a}}^e) dr \\
& = -(\mathbf{a}^e)^T \cdot 2 m_s V \int_0^l \mathbf{N}_s^T \mathbf{N}_{s,r} dr \cdot (\dot{\mathbf{a}}^e)
\end{aligned} \tag{10.30}$$

$$\begin{aligned}
& \int_0^l z(r) m_s \left(\frac{\partial^2 z}{\partial t^2} \right) dr = m_s \int_0^l z(r) \left(\frac{\partial^2 z}{\partial t^2} \right) dr = m_s \int_0^l z(r) \left(\frac{\partial^2 z}{\partial t^2} \right) dr = m_s \int_0^l (\mathbf{N}_s \mathbf{a}^e)^T (\mathbf{N}_s \ddot{\mathbf{a}}^e) dr \\
& = (\mathbf{a}^e)^T \cdot m_s \int_0^l \mathbf{N}_s^T \mathbf{N}_s dr \cdot (\ddot{\mathbf{a}}^e)
\end{aligned} \tag{10.31}$$

$$\begin{aligned}
\int_0^l z(r)c_s \left(\frac{\partial z}{\partial t} \right) dr &= c_s \int_0^l z(r) \left(\frac{\partial z}{\partial t} \right) dr = c_s \int_0^l (\mathbf{N}_s \mathbf{a}^e)^T (\mathbf{N}_s \dot{\mathbf{a}}^e) dr \\
&= (\mathbf{a}^e)^T \cdot c_s \int_0^l \mathbf{N}_s^T \mathbf{N}_s dr \cdot (\dot{\mathbf{a}}^e)
\end{aligned} \tag{10.32}$$

$$\begin{aligned}
-\int_0^l z(r)c_s V \left(\frac{\partial z}{\partial r} \right) dr &= -c_s V \int_0^l z(r) \left(\frac{\partial z}{\partial r} \right) dr \\
&= -c_s V \int_0^l (\mathbf{N}_s \mathbf{a}^e)^T (\mathbf{N}_{s,r} \mathbf{a}^e) dr = -(\mathbf{a}^e)^T \cdot c_s V \int_0^l \mathbf{N}_s^T \mathbf{N}_{s,r} dr \cdot (\mathbf{a}^e)
\end{aligned} \tag{10.33}$$

$$\begin{aligned}
-\int_0^l z(r)c_s \left(\frac{\partial y}{\partial t} \right) dr &= -c_s \int_0^l z(r) \left(\frac{\partial y}{\partial t} \right) dr \\
&= -c_s \int_0^l (\mathbf{N}_s \mathbf{a}^e)^T (\mathbf{N}_h \dot{\mathbf{a}}^e) dr = -(\mathbf{a}^e)^T \cdot c_s \int_0^l \mathbf{N}_s^T \mathbf{N}_h dr \cdot (\dot{\mathbf{a}}^e)
\end{aligned} \tag{10.34}$$

$$\begin{aligned}
\int_0^l z(r)c_s V \left(\frac{\partial y}{\partial r} \right) dr &= c_s V \int_0^l z(r) \left(\frac{\partial y}{\partial r} \right) dr \\
&= c_s V \int_0^l (\mathbf{N}_s \mathbf{a}^e)^T (\mathbf{N}_{h,r} \mathbf{a}^e) dr = (\mathbf{a}^e)^T \cdot c_s V \int_0^l \mathbf{N}_s^T \mathbf{N}_{h,r} dr \cdot (\mathbf{a}^e)
\end{aligned} \tag{10.35}$$

$$\begin{aligned}
-\int_0^l z(r)c_r \left(\frac{\partial w}{\partial t} \right) dr &= -c_r \int_0^l z(r) \left(\frac{\partial w}{\partial t} \right) dr \\
&= -c_r \int_0^l (\mathbf{N}_s \mathbf{a}^e)^T (\mathbf{N}_r \dot{\mathbf{a}}^e) dr = -(\mathbf{a}^e)^T \cdot c_r \int_0^l \mathbf{N}_s^T \mathbf{N}_r dr \cdot (\dot{\mathbf{a}}^e)
\end{aligned} \tag{10.36}$$

$$\begin{aligned}
\int_0^l z(r) c_r V \left(\frac{\partial w}{\partial r} \right) dr &= c_r V \int_0^l z(r) \left(\frac{\partial w}{\partial r} \right) dr \\
&= c_r V \int_0^l (\mathbf{N}_s \mathbf{a}^e)^T (\mathbf{N}_{r,r} \mathbf{a}^e) dr = (\mathbf{a}^e)^T \cdot c_r V \int_0^l \mathbf{N}_s^T \mathbf{N}_{r,r} dr \cdot (\mathbf{a}^e)
\end{aligned} \tag{10.37}$$

$$\begin{aligned}
\int_0^l z(r) c_r \left(\frac{\partial z}{\partial t} \right) dr &= c_r \int_0^l z(r) \left(\frac{\partial z}{\partial t} \right) dr \\
&= c_r \int_0^l (\mathbf{N}_s \mathbf{a}^e)^T (\mathbf{N}_s \dot{\mathbf{a}}^e) dr = (\mathbf{a}^e)^T \cdot c_r \int_0^l \mathbf{N}_s^T \mathbf{N}_s dr \cdot (\dot{\mathbf{a}}^e)
\end{aligned} \tag{10.38}$$

$$\begin{aligned}
-\int_0^l z(r) c_r V \left(\frac{\partial z}{\partial r} \right) dr &= -c_r V \int_0^l z(r) \left(\frac{\partial z}{\partial r} \right) dr \\
&= -c_r V \int_0^l (\mathbf{N}_s \mathbf{a}^e)^T (\mathbf{N}_{s,r} \mathbf{a}^e) dr = -(\mathbf{a}^e)^T \cdot c_r V \int_0^l \mathbf{N}_s^T \mathbf{N}_{s,r} dr \cdot (\mathbf{a}^e)
\end{aligned} \tag{10.39}$$

$$\begin{aligned}
\int_0^l z(r) k_s z(r) dr &= k_s \int_0^l z(r)^2 dr \\
&= k_s \int_0^l (\mathbf{N}_s \mathbf{a}^e)^T (\mathbf{N}_s \mathbf{a}^e) dr = (\mathbf{a}^e)^T \cdot k_s \int_0^l \mathbf{N}_s^T \mathbf{N}_s dr \cdot (\mathbf{a}^e)
\end{aligned} \tag{10.40}$$

$$\begin{aligned}
-\int_0^l z(r) k_s y(r) dr &= -k_s \int_0^l z(r) y(r) dr \\
&= -k_s \int_0^l (\mathbf{N}_s \mathbf{a}^e)^T (\mathbf{N}_h \mathbf{a}^e) dr = -(\mathbf{a}^e)^T \cdot k_s \int_0^l \mathbf{N}_s^T \mathbf{N}_h dr \cdot (\mathbf{a}^e)
\end{aligned} \tag{10.41}$$

$$\begin{aligned}
-\int_0^l z(r)k_r w(r)dr &= -k_r \int_0^l z(r)w(r)dr \\
&= -k_r \int_0^l (N_s \mathbf{a}^e)^T (N_r \mathbf{a}^e) dr = -(\mathbf{a}^e)^T \cdot k_r \int_0^l N_s^T N_r dr \cdot (\mathbf{a}^e)
\end{aligned} \tag{10.42}$$

$$\begin{aligned}
\int_0^l z(r)k_r z(r)dr &= k_r \int_0^l z(r)^2 dr \\
&= k_r \int_0^l (N_s \mathbf{a}^e)^T (N_s \mathbf{a}^e) dr = (\mathbf{a}^e)^T \cdot k_r \int_0^l N_s^T N_s dr \cdot (\mathbf{a}^e)
\end{aligned} \tag{10.43}$$

By using the principle of the energy, the second-layer beam's mass, damping, and stiffness matrices of the slab track element in a moving frame of reference can be obtained as follows:

$$\mathbf{m}_s^e = m_s \int_0^l N_s^T N_s dr \tag{10.44}$$

$$\begin{aligned}
\mathbf{c}_s^e &= -2m_s V \int_0^l N_s^T N_{s,r} dr + c_s \int_0^l N_s^T N_s dr \\
&\quad - c_s \int_0^l N_s^T N_h dr - c_r \int_0^l N_s^T N_r dr + c_r \int_0^l N_s^T N_s dr
\end{aligned} \tag{10.45}$$

$$\begin{aligned}
\mathbf{k}_s^e &= E_s I_s \int_0^l N_{s,rr}^T N_{s,rr} dr - m_s V^2 \int_0^l N_{s,r}^T N_{s,r} dr \\
&\quad - c_s V \int_0^l N_s^T N_{s,r} dr + c_s V \int_0^l N_s^T N_{h,r} dr + c_r V \int_0^l N_s^T N_{r,r} dr \\
&\quad - c_r V \int_0^l N_s^T N_{s,r} dr + k_s \int_0^l N_s^T N_s dr - k_s \int_0^l N_s^T N_h dr \\
&\quad - k_r \int_0^l N_s^T N_r dr + k_r \int_0^l N_s^T N_s dr
\end{aligned} \tag{10.46}$$

10.2.2.3 The Third Layer Beam's Matrix of the Slab Track Element in a Moving Frame of Reference

The governing equation (10.7) is multiplied by a weighting function (variation) y , and then integrated over the element length, leading to the variational (or weak) form as follows:

$$\int_0^l y(r) \left\{ E_h I_h \frac{\partial^4 y}{\partial r^4} + m_h \left[V^2 \left(\frac{\partial^2 y}{\partial r^2} \right) - 2V \left(\frac{\partial^2 y}{\partial r \partial t} \right) + \left(\frac{\partial^2 y}{\partial t^2} \right) \right] + c_h \left[\left(\frac{\partial y}{\partial r} \right) - V \left(\frac{\partial y}{\partial t} \right) \right] - c_s \left[\left(\frac{\partial z}{\partial t} \right) - V \left(\frac{\partial z}{\partial r} \right) \right] + c_s \left[\left(\frac{\partial y}{\partial t} \right) - V \left(\frac{\partial y}{\partial r} \right) \right] + k_h y - k_s (z - y) \right\} dr = 0 \quad (10.47)$$

Take the integration to each term of above equation by parts over the element length l , namely:

$$\begin{aligned} \int_0^l y(r) E_h I_h \left(\frac{\partial^4 y}{\partial r^4} \right) dr &= E_h I_h \int_0^l y(r) d \left(\frac{\partial^3 y}{\partial r^3} \right) \\ &= E_h I_h \left[\left(y(r) \cdot \frac{\partial^3 y}{\partial r^3} \right)_o^l - \int_0^l \frac{\partial^3 y}{\partial r^3} \cdot \frac{\partial y}{\partial r} dr \right] = -E_h I_h \int_0^l \frac{\partial y}{\partial r} d \left(\frac{\partial^2 y}{\partial r^2} \right) \\ &= -E_h I_h \left[\left(\frac{\partial y}{\partial r} \cdot \frac{\partial^2 y}{\partial r^2} \right)_o^l - \int_0^l \frac{\partial^2 y}{\partial r^2} \cdot \frac{\partial^2 y}{\partial r^2} dr \right] \\ &= E_h I_h \int_0^l (\mathbf{N}_{h,r} \mathbf{a}^e)^T (\mathbf{N}_{h,r} \mathbf{a}^e) dr = (\mathbf{a}^e)^T \cdot E_h I_h \int_0^l \mathbf{N}_{h,r}^T \mathbf{N}_{h,r} dr \cdot (\mathbf{a}^e) \end{aligned} \quad (10.48)$$

$$\begin{aligned} \int_0^l y(r) m_h V^2 \left(\frac{\partial^2 y}{\partial r^2} \right) dr &= m_h V^2 \int_0^l y(r) \left(\frac{\partial^2 y}{\partial r^2} \right) dr \\ &= m_h V^2 \int_0^l y(r) d \left(\frac{\partial y}{\partial r} \right) = m_h V^2 \left[\left(y(r) \cdot \frac{\partial y}{\partial r} \right)_o^l - \int_0^l \frac{\partial y}{\partial r} \cdot \frac{\partial y}{\partial r} dr \right] \\ &= -m_h V^2 \int_0^l (\mathbf{N}_{h,r} \mathbf{a}^e)^T (\mathbf{N}_{h,r} \mathbf{a}^e) dr = -(\mathbf{a}^e)^T \cdot m_h V^2 \int_0^l \mathbf{N}_{h,r}^T \mathbf{N}_{h,r} dr \cdot (\mathbf{a}^e) \end{aligned} \quad (10.49)$$

$$\begin{aligned}
-2 \int_0^l m_h V y(r) \left(\frac{\partial^2 y}{\partial r \partial t} \right) dr &= -2m_h V \int_0^l y(r) \left(\frac{\partial^2 y}{\partial r \partial t} \right) dr = -2m_h V \int_0^l (\mathbf{N}_h \mathbf{a}^e)^T (\mathbf{N}_{h,r} \dot{\mathbf{a}}^e) dr \\
&= -(\mathbf{a}^e)^T \cdot 2m_h V \int_0^l \mathbf{N}_h^T \mathbf{N}_{h,r} dr \cdot (\dot{\mathbf{a}}^e)
\end{aligned} \tag{10.50}$$

$$\begin{aligned}
\int_0^l y(r) m_h \left(\frac{\partial^2 y}{\partial t^2} \right) dr &= m_h \int_0^l y(r) \left(\frac{\partial^2 y}{\partial t^2} \right) dr \\
&= m_h \int_0^l y(r) \left(\frac{\partial^2 y}{\partial t^2} \right) dr = m_h \int_0^l (\mathbf{N}_h \mathbf{a}^e)^T (\mathbf{N}_h \ddot{\mathbf{a}}^e) dr \\
&= (\mathbf{a}^e)^T \cdot m_h \int_0^l \mathbf{N}_h^T \mathbf{N}_h dr \cdot (\ddot{\mathbf{a}}^e)
\end{aligned} \tag{10.51}$$

$$\begin{aligned}
\int_0^l y(r) c_h \left(\frac{\partial y}{\partial t} \right) dr &= c_h \int_0^l y(r) \left(\frac{\partial y}{\partial t} \right) dr \\
&= c_h \int_0^l (\mathbf{N}_h \mathbf{a}^e)^T (\mathbf{N}_h \dot{\mathbf{a}}^e) dr = (\mathbf{a}^e)^T \cdot c_h \int_0^l \mathbf{N}_h^T \mathbf{N}_h dr \cdot (\dot{\mathbf{a}}^e)
\end{aligned} \tag{10.52}$$

$$\begin{aligned}
-\int_0^l y(r) c_h V \left(\frac{\partial y}{\partial r} \right) dr &= -c_h V \int_0^l y(r) \left(\frac{\partial y}{\partial r} \right) dr \\
&= -c_h V \int_0^l (\mathbf{N}_h \mathbf{a}^e)^T (\mathbf{N}_{h,r} \mathbf{a}^e) dr \\
&= -(\mathbf{a}^e)^T \cdot c_h V \int_0^l \mathbf{N}_h^T \mathbf{N}_{h,r} dr \cdot (\mathbf{a}^e)
\end{aligned} \tag{10.53}$$

$$\begin{aligned}
-\int_0^l y(r)c_s\left(\frac{\partial z}{\partial t}\right)dr &= -c_s\int_0^l y(r)\left(\frac{\partial z}{\partial t}\right)dr \\
&= -c_s\int_0^l (\mathbf{N}_h\mathbf{a}^e)^T(\mathbf{N}_s\dot{\mathbf{a}}^e)dr = -(\mathbf{a}^e)^T\cdot c_s\int_0^l \mathbf{N}_h^T\mathbf{N}_sdr\cdot(\dot{\mathbf{a}}^e)
\end{aligned} \tag{10.54}$$

$$\begin{aligned}
\int_0^l y(r)c_sV\left(\frac{\partial z}{\partial r}\right)dr &= c_sV\int_0^l y(r)\left(\frac{\partial z}{\partial r}\right)dr \\
&= c_sV\int_0^l (\mathbf{N}_h\mathbf{a}^e)^T(\mathbf{N}_{s,r}\mathbf{a}^e)dr = (\mathbf{a}^e)^T\cdot c_sV\int_0^l \mathbf{N}_h^T\mathbf{N}_{s,r}dr\cdot(\mathbf{a}^e)
\end{aligned} \tag{10.55}$$

$$\begin{aligned}
\int_0^l y(r)c_s\left(\frac{\partial y}{\partial t}\right)dr &= c_s\int_0^l y(r)\left(\frac{\partial y}{\partial t}\right)dr \\
&= c_s\int_0^l (\mathbf{N}_h\mathbf{a}^e)^T(\mathbf{N}_h\dot{\mathbf{a}}^e)dr = (\mathbf{a}^e)^T\cdot c_s\int_0^l \mathbf{N}_h^T\mathbf{N}_hdr\cdot(\dot{\mathbf{a}}^e)
\end{aligned} \tag{10.56}$$

$$\begin{aligned}
-\int_0^l y(r)c_sV\left(\frac{\partial y}{\partial r}\right)dr &= -c_sV\int_0^l y(r)\left(\frac{\partial y}{\partial r}\right)dr \\
&= -c_sV\int_0^l (\mathbf{N}_h\mathbf{a}^e)^T(\mathbf{N}_{h,r}\mathbf{a}^e)dr = -(\mathbf{a}^e)^T\cdot c_sV\int_0^l \mathbf{N}_h^T\mathbf{N}_{h,r}dr\cdot(\mathbf{a}^e)
\end{aligned} \tag{10.57}$$

$$\begin{aligned}
\int_0^l y(r)k_hy(r)dr &= k_h\int_0^l y(r)^2dr = k_h\int_0^l (\mathbf{N}_h\mathbf{a}^e)^T(\mathbf{N}_h\mathbf{a}^e)dr \\
&= (\mathbf{a}^e)^T\cdot k_h\int_0^l \mathbf{N}_h^T\mathbf{N}_hdr\cdot(\mathbf{a}^e)
\end{aligned} \tag{10.58}$$

$$\begin{aligned}
-\int_0^l y(r)k_s z(r)dr &= -k_s \int_0^l y(r)z(r)dr \\
&= -k_s \int_0^l (\mathbf{N}_h \mathbf{a}^e)^T (\mathbf{N}_s \mathbf{a}^e) dr = -(\mathbf{a}^e)^T \cdot k_s \int_0^l \mathbf{N}_h^T \mathbf{N}_s dr \cdot (\mathbf{a}^e)
\end{aligned} \tag{10.59}$$

$$\begin{aligned}
\int_0^l y(r)k_s y(r)dr &= k_s \int_0^l y(r)^2 dr = k_s \int_0^l (\mathbf{N}_h \mathbf{a}^e)^T (\mathbf{N}_h \mathbf{a}^e) dr \\
&= (\mathbf{a}^e)^T \cdot k_s \int_0^l \mathbf{N}_h^T \mathbf{N}_h dr \cdot (\mathbf{a}^e)
\end{aligned} \tag{10.60}$$

By using the principle of the energy, the third layer beam's mass, damping, and stiffness matrices of the slab track element in a moving frame of reference can be obtained as follows:

$$\mathbf{m}_h^e = m_h \int_0^l \mathbf{N}_h^T \mathbf{N}_h dr \tag{10.61}$$

$$\mathbf{c}_h^e = -2m_h V \int_0^l \mathbf{N}_h^T \mathbf{N}_{h,r} dr + c_h \int_0^l \mathbf{N}_h^T \mathbf{N}_h dr - c_s \int_0^l \mathbf{N}_h^T \mathbf{N}_s dr + c_s \int_0^l \mathbf{N}_h^T \mathbf{N}_h dr \tag{10.62}$$

$$\begin{aligned}
\mathbf{k}_h^e &= E_h I_h \int_0^l \mathbf{N}_{h,rr}^T \mathbf{N}_{h,rr} dr - m_h V^2 \int_0^l \mathbf{N}_{h,r}^T \mathbf{N}_{h,r} dr \\
&\quad - c_h V \int_0^l \mathbf{N}_h^T \mathbf{N}_{h,r} dr + c_s V \int_0^l \mathbf{N}_h^T \mathbf{N}_{s,r} dr \\
&\quad - c_s V \int_0^l \mathbf{N}_h^T \mathbf{N}_{h,r} dr + k_h \int_0^l \mathbf{N}_h^T \mathbf{N}_h dr - k_s \int_0^l \mathbf{N}_h^T \mathbf{N}_s dr + k_s \int_0^l \mathbf{N}_h^T \mathbf{N}_h dr
\end{aligned} \tag{10.63}$$

Finally, the mass, damping, and stiffness matrices of the slab track element in a moving frame of reference are as follows:

$$\mathbf{m}_1^e = \mathbf{m}_r^e + \mathbf{m}_s^e + \mathbf{m}_h^e \quad (10.64)$$

$$\mathbf{c}_1^e = \mathbf{c}_r^e + \mathbf{c}_s^e + \mathbf{c}_h^e \quad (10.65)$$

$$\mathbf{k}_1^e = \mathbf{k}_r^e + \mathbf{k}_s^e + \mathbf{k}_h^e \quad (10.66)$$

Based on the finite element assembling rule, the global mass matrix, the global damping matrix, and the global stiffness matrix of the slab track element in a moving frame of reference can be obtained by assembling the element mass matrix (10.64), the element damping matrix (10.65), and the element stiffness matrix (10.66).

$$\mathbf{m}_1 = \sum_e \mathbf{m}_1^e, \quad \mathbf{c}_1 = \sum_e \mathbf{c}_1^e, \quad \mathbf{k}_1 = \sum_e \mathbf{k}_1^e \quad (10.67)$$

By using Lagrange equation, the finite element equation of the slab track structure in a moving frame of reference can be obtained as follows:

$$\mathbf{m}_1 \ddot{\mathbf{a}}_1 + \mathbf{c}_1 \dot{\mathbf{a}}_1 + \mathbf{k}_1 \mathbf{a}_1 = \mathbf{Q}_1 \quad (10.68)$$

where \mathbf{Q}_1 is the global nodal load vector of the slab track structure.

10.3 Vehicle Element Model

Vehicle element model here is the same as the one in Fig. 9.4 of the Chap. 9. The stiffness matrix (\mathbf{k}_u^e), the mass matrix (\mathbf{m}_u^e), the damping matrix (\mathbf{c}_u^e), and the nodal load vector (\mathbf{Q}_u^e) of the vehicle element can refer to (9.58), (9.71), (9.74) and (9.59), respectively.

10.4 Finite Element Equation of the Vehicle-Slab Track Coupling System

Considering that the finite element equation of the vehicle and slab track coupling system consists of two elements, namely the slab track element and the vehicle element, of which the stiffness matrix, the mass matrix, and the damping matrix of the slab track element are \mathbf{k}_1^e , \mathbf{m}_1^e , \mathbf{c}_1^e , respectively, with a calculating formula illustrated in 10.2; while the stiffness matrix, the mass matrix, and the damping matrix of the vehicle element are \mathbf{k}_u^e , \mathbf{m}_u^e , \mathbf{c}_u^e , respectively, shown in (9.58), (9.71) and (9.74) in Chap. 9. In numerical calculation, it only needs to assemble the global

stiffness matrix, the global mass matrix, the global damping matrix, and the global load vector of the track structure once. And in each following calculating time step, by assembling the stiffness matrix, the mass matrix, the damping matrix, and the load vector of the vehicle element into the global stiffness matrix, the global mass matrix, the global damping matrix, and the global load vector of track structure with the standard finite element assembling rule, one can obtain the global stiffness matrix, the global mass matrix, the global damping matrix, and the global load vector of the vehicle-slab track coupling system.

Therefore, the dynamic finite element equation of the vehicle-slab track coupling system is as follows:

$$M\ddot{a} + C\dot{a} + Ka = Q \quad (10.69)$$

where M , C , K , and Q are the global mass matrix, the global damping matrix, the global stiffness matrix, and the global load vector of the vehicle-slab track coupling system, respectively.

$$\begin{aligned} M &= \sum_e (m_1 + m_u^e), & C &= \sum_e (c_1 + c_u^e), & K &= \sum_e (k_1 + k_u^e), \\ Q &= \sum_e (Q_1 + Q_u^e) \end{aligned} \quad (10.70)$$

The numerical solution to the dynamic finite element equation of the vehicle-slab track coupling system can be achieved by the direct integration method, such as Newmark's integration method.

10.5 Algorithm Verification

According to the above algorithm, the computational program FEST (Finite Element program for the Slab Track) is developed by using MATLAB. In order to verify the correctness of the model and the algorithm of this chapter, let us investigate the dynamic response of the vehicle and the track structure for Chinese high-speed train CRH3 running through the CRTS II slab track with the speed of 72 km/h. The calculated results are compared with those by conventional finite element method. Assuming that the railway is completely smooth, the computational time step is 0.001 s. Parameters of the Chinese high-speed train CRH3 and the CRTS II slab track structure are listed in Tables 6.7 and 10.1. The results are shown in Figs. 10.6 and 10.7, in which Fig. 10.6 is the distribution of the rail displacement along the track direction, and Fig. 10.7 is the time history of the wheel-rail contact force.

Table 10.1 Parameters of CRTS II slab track structure

Parameters	Values	Parameters	Values
Rail elasticity modulus/(MPa)	2.1×10^5	Inertia moment of concrete support layer/(m^4)	3.3×10^{-3}
Rail inertia moment/(m^4)	3.217×10^{-5}	Stiffness of rail pads and fasteners/(MN/m)	60
Rail mass/(kg/m)	60	Damping of rail pads and fasteners/(kN s/m)	47.7
Mass of track slab/(kg/m)	1275	CA mortar stiffness/(MN/m)	900
Elasticity modulus of track slab/(MPa)	3.9×10^4	CA mortar damping/(kN s/m)	83
Inertia moment of track slab/(m^4)	8.5×10^{-5}	Subgrade stiffness/(MN/m)	60
Mass of concrete support layer/(kg/m)	2340	Subgrade damping/(kN s/m)	90
Elasticity modulus of concrete support layer/(MPa)	3×10^4	Element length/(m)	0.5

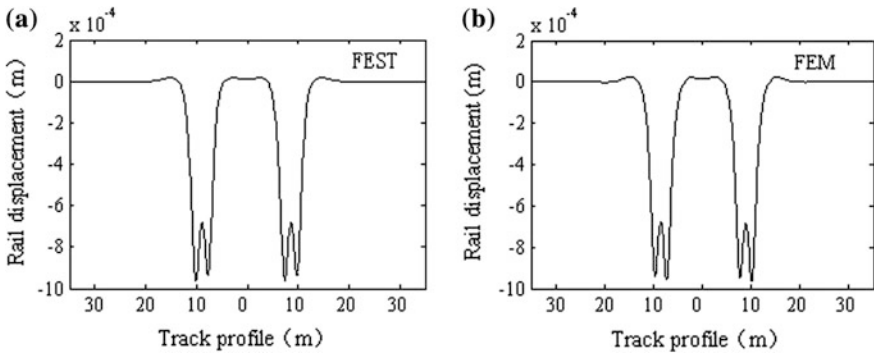


Fig. 10.6 Rail vertical displacement distribution along the track direction. **a** Calculated results with FEST approach and **b** calculated results with FEM approach

As illustrated in Fig. 10.6, the rail vertical displacements obtained by using the model and the algorithm presented in this chapter are in good agreement with those by the conventional finite element method [11]. Figure 10.7 is the time history of the wheel-rail contact force by the two methods. Due to the differences between the two algorithms and the influence of the initial computational conditions, the curves of the calculated results before stability are different, but in the end they all converge to the static load value exerted on the wheels. Since the track is assumed to be completely smooth, it shows that the calculated results are accurate and thus proves the correctness and feasibility of the model and the algorithm.

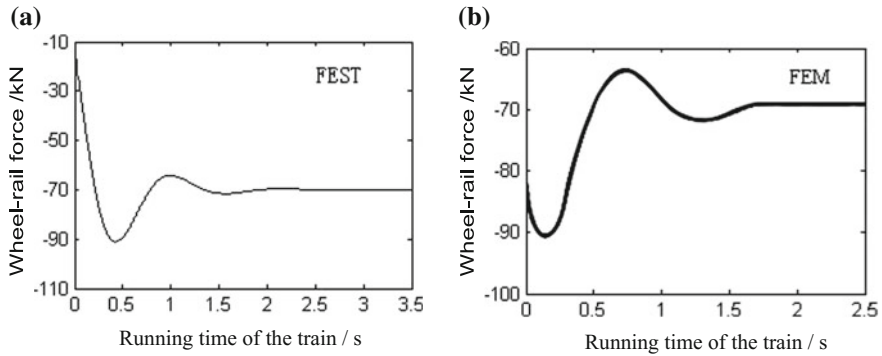


Fig. 10.7 Time history of the wheel-rail contact force. **a** Wheel-rail contact force with FEST approach and **b** wheel-rail contact force with FEM approach

10.6 Dynamic Analysis of High-Speed Train and Slab Track Coupling System

As an application example, dynamic analysis of the high-speed train and the slab track coupling system is carried out by the presented model and algorithm. The vehicle is Chinese high-speed train CRH3; the track structure is CRTS II slab track at the subgrade section, as shown in Figs. 10.8 and 10.9, respectively. The vehicle parameters and the track parameters are as shown in Tables 6.7 and 10.1. The train speed 200 km/h is specified. The German low interference spectrum for high-speed railway is adopted to simulate the track irregularity as shown in Fig. 10.10. Take the time step as 0.001 s in calculation. Because of the influence of the initial conditions, the calculated results of the first few seconds are usually inaccurate. The following is the time history of dynamic response within 5 s after the calculation is stable, including the acceleration of the car body, the displacement of the rail, the

Fig. 10.8 Chinese high-speed train CRH3





Fig. 10.9 Slab track of high-speed railway at the subgrade section

track slab, and the concrete support layer, and their corresponding velocity and acceleration, as well as the wheel-rail contact force [11, 12].

The interaction between the wheel and the rail increases significantly because of the random irregularities of the track. Figures 10.11, 10.12 and 10.13 demonstrate the time history curves of the vertical displacements of the rail, the track slab, and the concrete support layer at the second wheel-rail contact point, respectively. Because of the random irregularities of the track, the displacements of the rail, the track slab, and the concrete support layer are oscillating.

Figures 10.14, 10.15 and 10.16 show the vertical displacement distributions of the rail, the track slab, and the concrete support layer along the track direction, respectively. In Fig. 10.14, there are four obvious peaks in the rail displacement diagram, corresponding to the four wheels' action points. In Fig. 10.15 there are only two pliable peaks in the track slab displacement diagram with the maximum amplitude much smaller than those in Fig. 10.14. The same situation for the

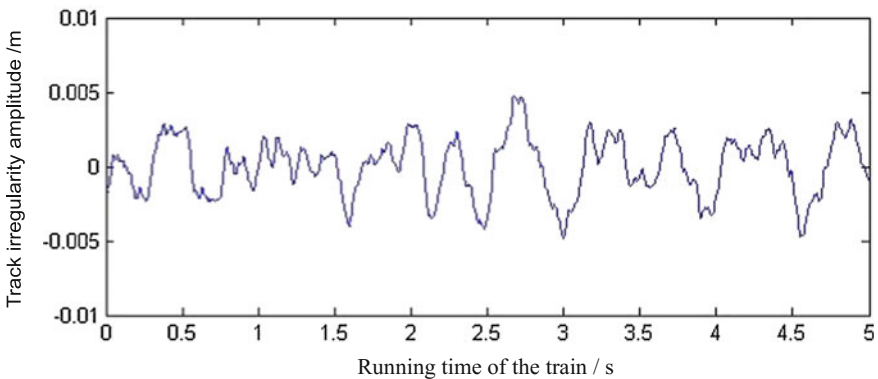


Fig. 10.10 Track irregularity sample with low interference spectrum in Germany

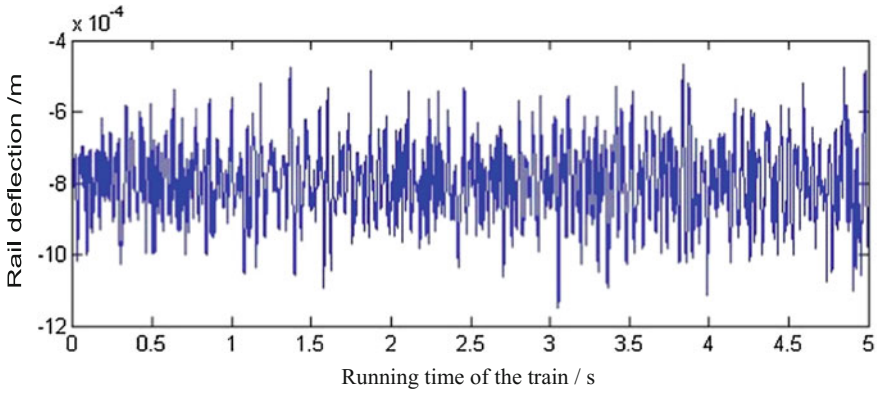


Fig. 10.11 Time history of the rail vertical displacement

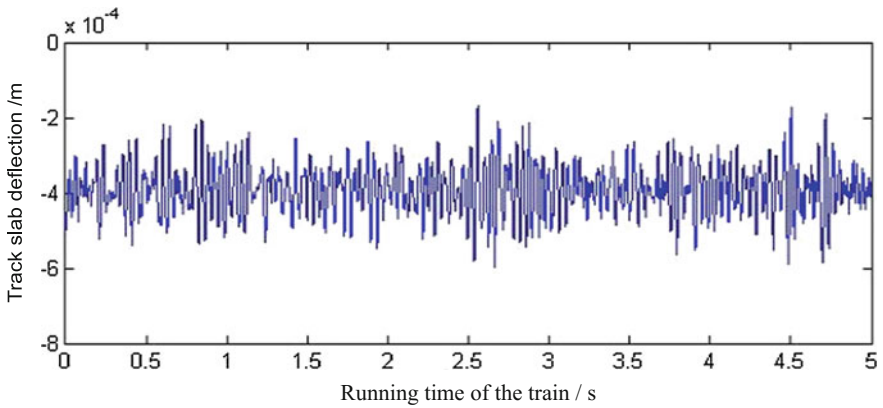


Fig. 10.12 Time history of the slab vertical displacement

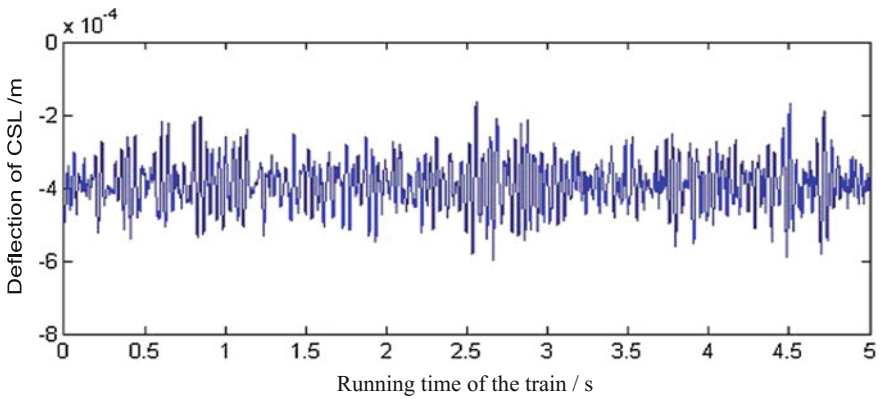


Fig. 10.13 Time history of the vertical displacement of the concrete support layer (CSL)

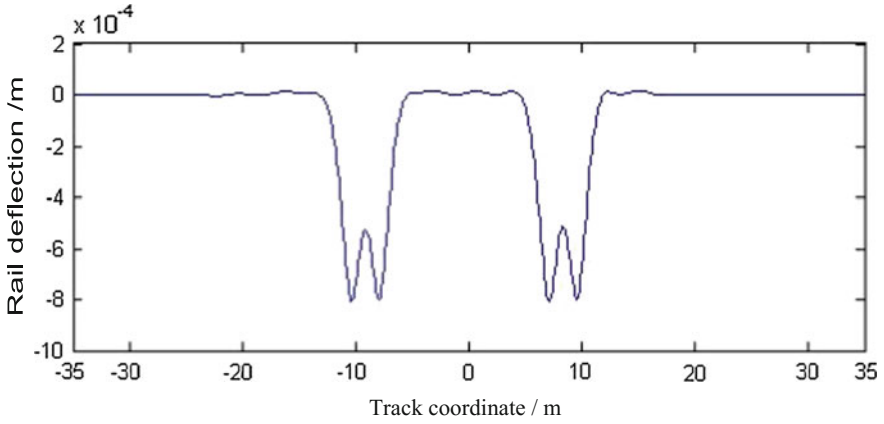


Fig. 10.14 Rail vertical displacement along the track direction

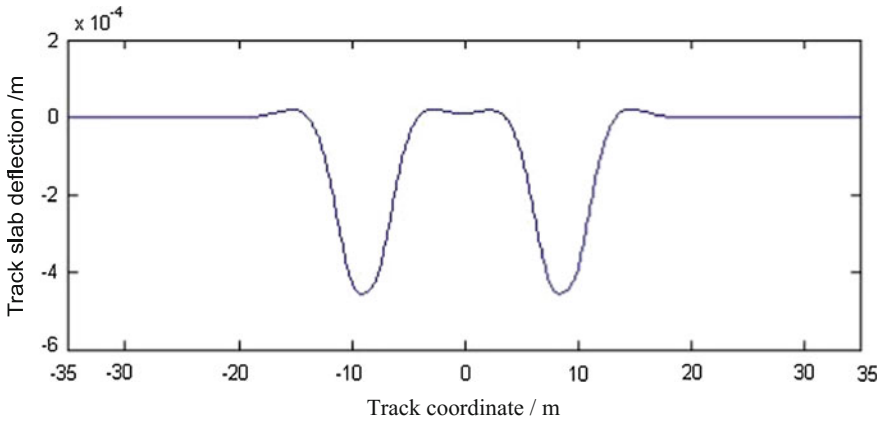


Fig. 10.15 Track slab vertical displacement along the track direction

displacement distribution of the concrete support layer also is observed in Fig. 10.16, which illustrates the additional dynamic load induced by the train operation that is obviously reduced due to the existing of the rail pads and fasteners and the CA mortar.

Figures 10.17, 10.18 and 10.19 represent the time history of the vertical velocity of the rail, the track slab, and the concrete support layer at the second wheel-rail contact point, respectively, which show the vibration velocities of the rail, the track slab, and the concrete support layer attenuating in turn. Figures 10.20, 10.21 and 10.22 are the time history of the vertical acceleration of the rail, the track slab, and the concrete support layer at the second wheel-rail contact point, respectively. Due

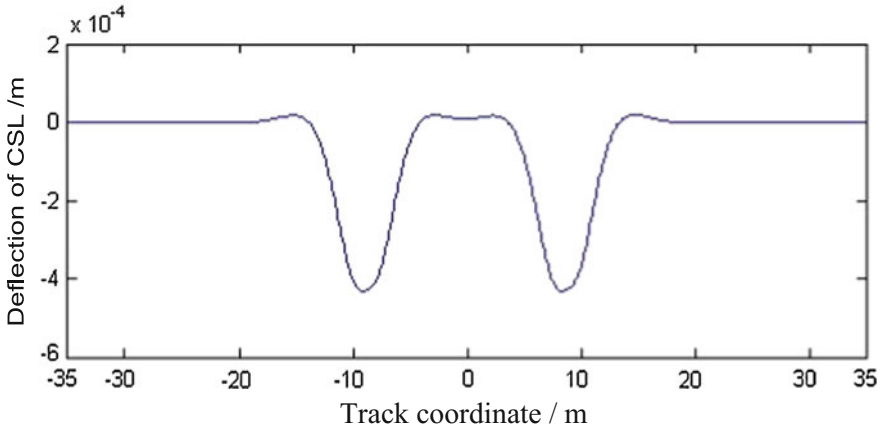


Fig. 10.16 Vertical displacement of the concrete support layer (CSL) along the track direction

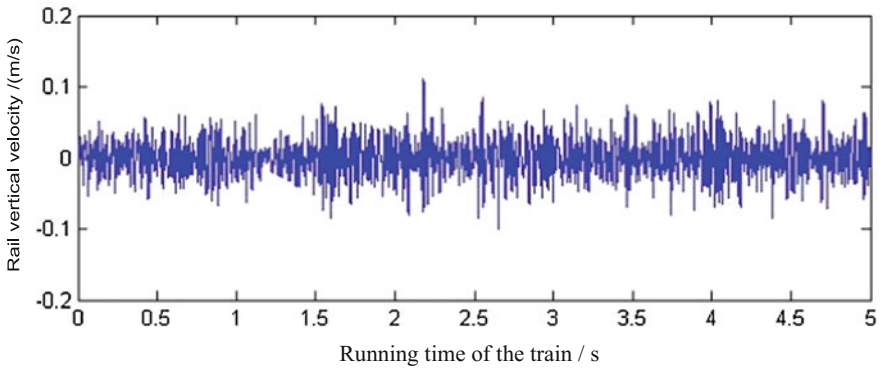


Fig. 10.17 Time history of the rail vertical velocity

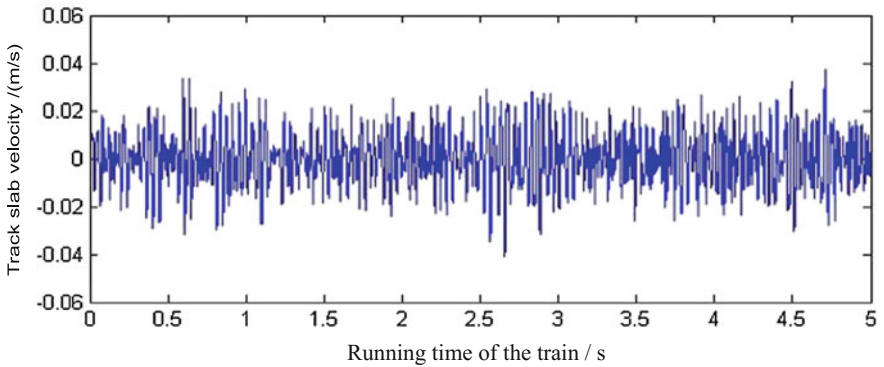


Fig. 10.18 Time history of the track slab vertical velocity

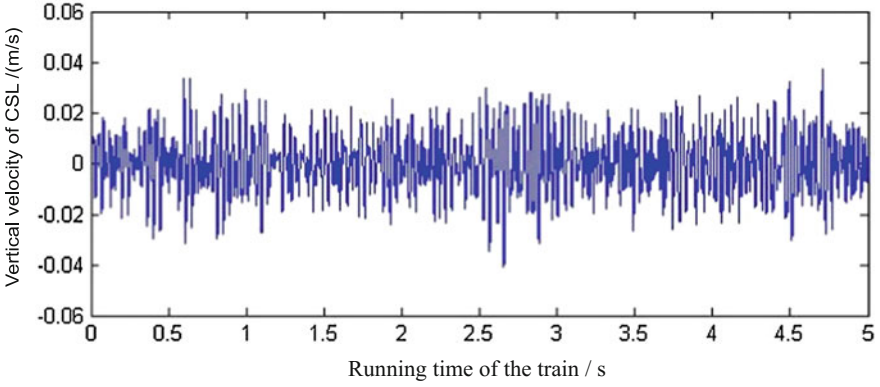


Fig. 10.19 Time history of the vertical velocity of the concrete support layer (CSL)

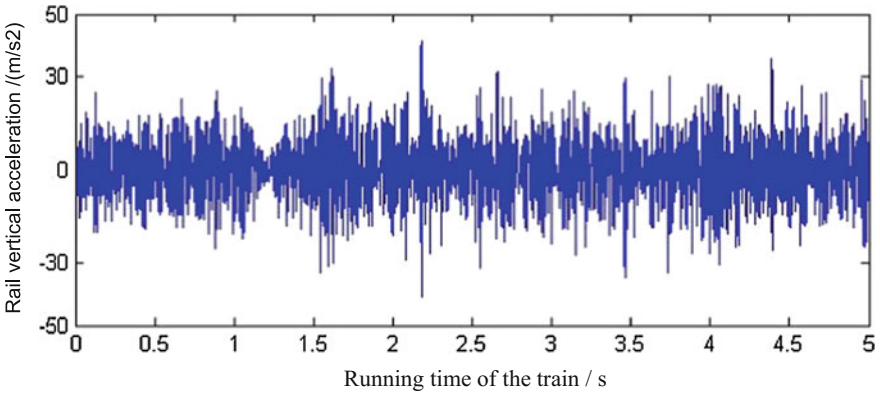


Fig. 10.20 Time history of the rail vertical acceleration

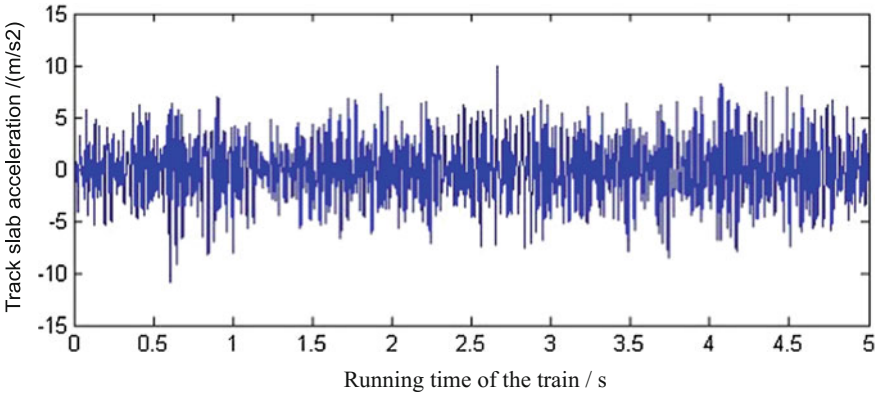


Fig. 10.21 Time history of the track slab vertical acceleration

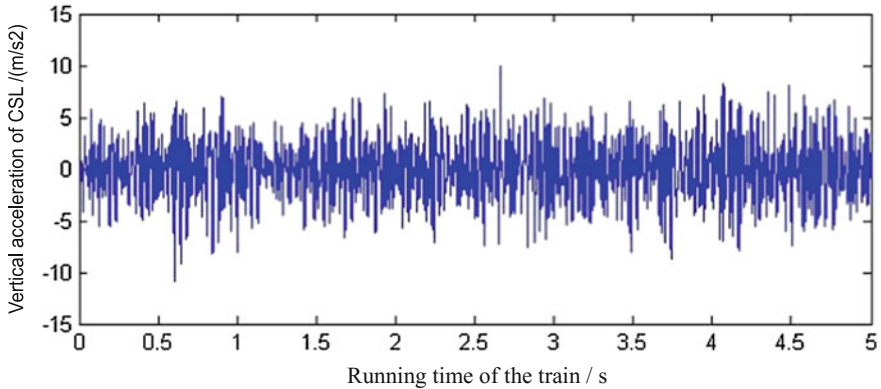


Fig. 10.22 Time history of the vertical acceleration of the concrete support layer (CSL)

to the existing of the rail pads and fasteners and the CA mortar, the acceleration peaks of the track slab and the concrete support layer are also reduced obviously.

Figure 10.23 shows the time history of the car body vibration acceleration. It is an important indicator of measuring passengers' riding comfort. As shown in this Figure, in case of the train speed of 200 m/h and the track irregularity generated by the German low interference spectrum for high-speed railway, the acceleration amplitude of the car body is in a reasonable range, which can guarantee the passengers' comfort.

Figure 10.24 is the time history of the wheel-rail contact force, from which it can be observed that the wheel-rail contact force fluctuates around the static load of 70 kN, with maximum peak not more than 120 kN.

As a conclusion, the slab track element model and the associated algorithm in a moving frame of reference for dynamic analysis of the vehicle-track coupling

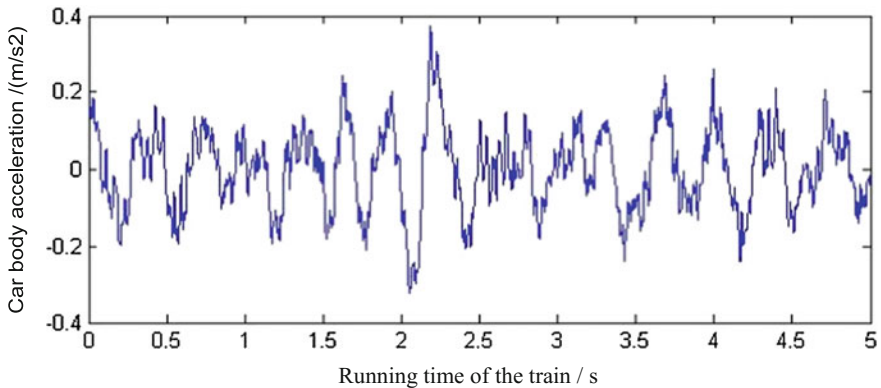


Fig. 10.23 Time history of the car body acceleration

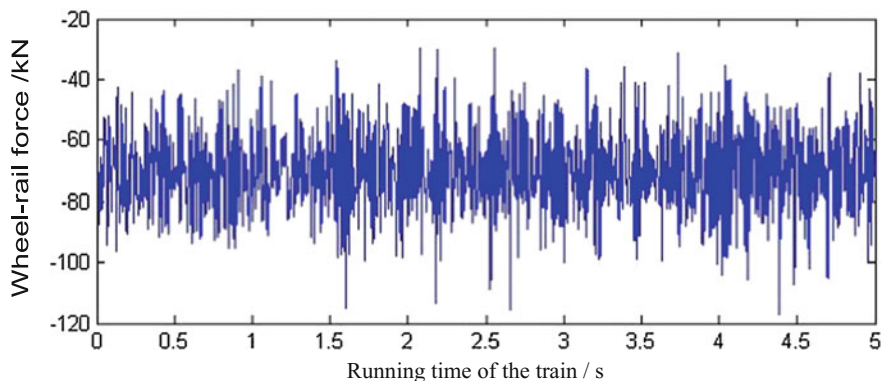


Fig. 10.24 Time history of the wheel-rail contact force

system are presented in this chapter. Three-layer continuous beam model for the slab track is developed, and the mass, damping, and stiffness matrices of the slab track element in a moving frame of reference are deduced. A whole vehicle is taken into account as a vehicle element with 26 degrees of freedom.

The main advantage of the approach is that, unlike in the FEM, the moving vehicle always acts at the same point in the numerical model, thereby eliminating the need for keeping track of the contact point with respect to individual elements. In addition, the moving vehicle will never run out of the truncated model. However, the defect is that the track structure has to be assumed continuous, which is different from the fact that the rail is supported by discrete supports.

References

1. Grassie SL, Gregory RW, Harrison D, Johnson KL (1982) The dynamic response of railway track to high frequency vertical excitation. *J Mech Eng Sci* 24:77–90
2. Eisenmann J (2002) Redundancy of Rheda-type slab track. *Eisenbahningenieur* 53(10):13–18
3. Zhai WM (1991) Vehicles-track vertical coupling dynamics. Doctor's dissertation of Southwest Jiaotong University, Chengdu
4. Zhai WM (1992) The vertical model of vehicle-track system and its coupling dynamics. *J China Railway Soc* 14(3):10–21
5. Xiang J, He D (2007) Analysis model of vertical vibration of high speed train and Bøgle slab track system. *J Traffic Transp Eng* 7(3): 1–5
6. He D, Xiang J, Zeng QY (2007) A new method for dynamics modeling of ballastless track. *J Central South Univ* 12(6):1206–1211
7. Lei XY, Sheng XZ (2008) Theoretical research on modern track, 2nd edn. China Railway Publishing House, Beijing
8. Lei XY, Zhang B, Liu QJ (2009) Model of vehicle and track elements for vertical dynamic analysis of vertical-track system. *J Vibr Shock* 29(3): 168–173
9. Xie WP, Zhen B (2005) Analysis of stable dynamic response of Winkler beam under moving load. *J Wuhan Univ Technol* 27(7):61–63

10. Koh CG, Ong JSY, Chua KH, D Feng J (2003) Moving element method for train—track dynamics. *Int J Numer Methods Eng* 56:1549–1567
11. Wang J (2012) Moving element method for high-speed railway ballastless track dynamic performance analysis. Master thesis. East China Jiaotong University, Nanchang
12. Lei XY, Wang J (2014) Dynamic analysis of the train and slab track coupling system with finite elements in a moving frame of reference. *J Vib Control* 20(9):1301–1317